Supplemental Figures with figure legends

Figure S1

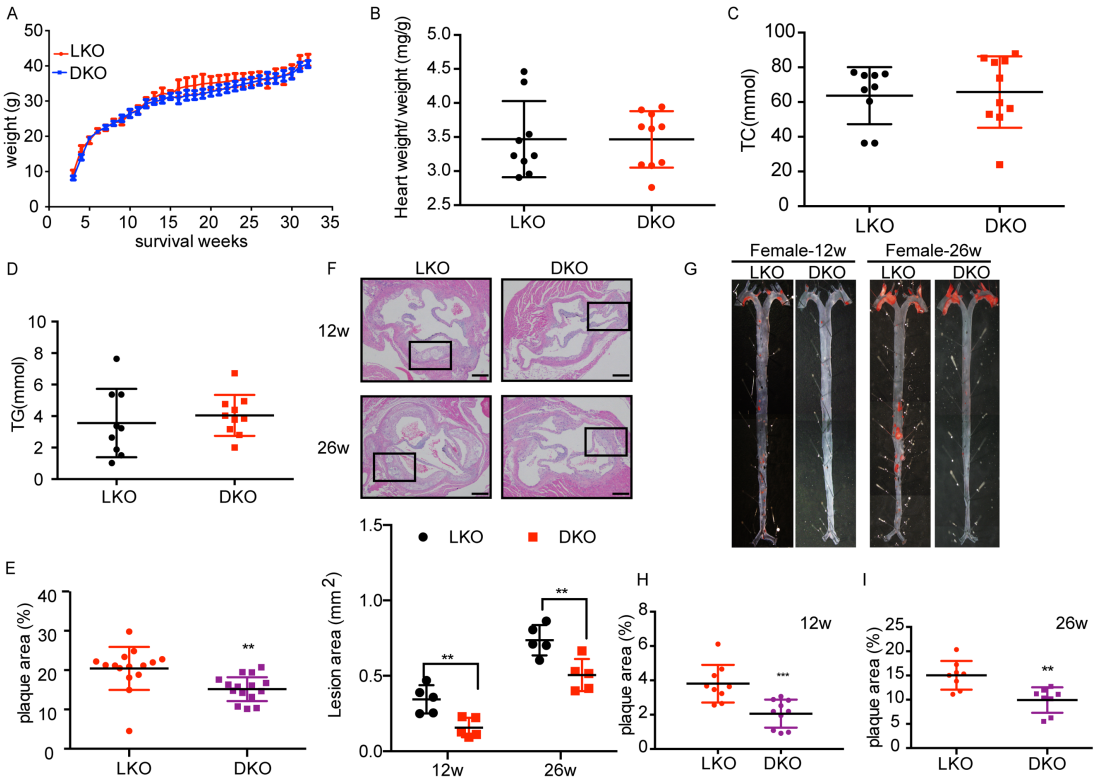

Supplemental Figure S1. Phenotypes of ALDH2 KO mice on LDLR and ~~*ApoE*~~ *APOE* background. A, Mouse body weights for LDLR KO and LDLR/ALDH2 DKO from 3 to 32 weeks (n=9-10); WD feeding started at age of week 6. **B,** Ratio of heart weight (mg)/body weight (g) for LDLR KO (n=9) and LDLR/ALDH2 DKO mice (n=10) after 26 weeks of WD feeding. **C to D,** triglycerides (TG) and total cholesterol (TC) in LDLR KO and LDLR/ALDH2 DKO mice fed WD for 26 weeks (n=9-10). **E,** ~~en face Sudan IV staining in LDLR KO mice fed WD for 26 weeks. **F,** en face Sudan IV staining in LDLR/ALDH2 DKO mice fed WD for 26 weeks. **G,**~~ quantification of Sudan IV-positive areas of aortas from male mice after 26w WD feeding in a duplicate study (n=15). **FH~~I~~,** aortic root lesions stained with H&E from male LDLR KO and LDLR/ALDH2 DKO mice (12w and 26w) (n=5). Scale bar, 400μm. **G to I,** representative en face Sudan IV staining and quantification of Sudan IV-positive areas of aortas from female mice after 12w WD feeding (H, n=10) and 26w WD (I, n=8) *LDLR*$^{-/-}$ (LKO) and *ALDH2*$^{-/-}$*LDLR*$^{-/-}$ (DKO) mice. ~~representative IHC and quantification of macrophages, collagen and SMCs after 12 weeks (n=8-9). Scale bar, 400μm.~~ Statistical comparisons were made

using 2-tailed Student's t test. All data represent mean ± SDEM. *P < 0.05, **P < 0.01, ***P < 0.001.

Figure S2

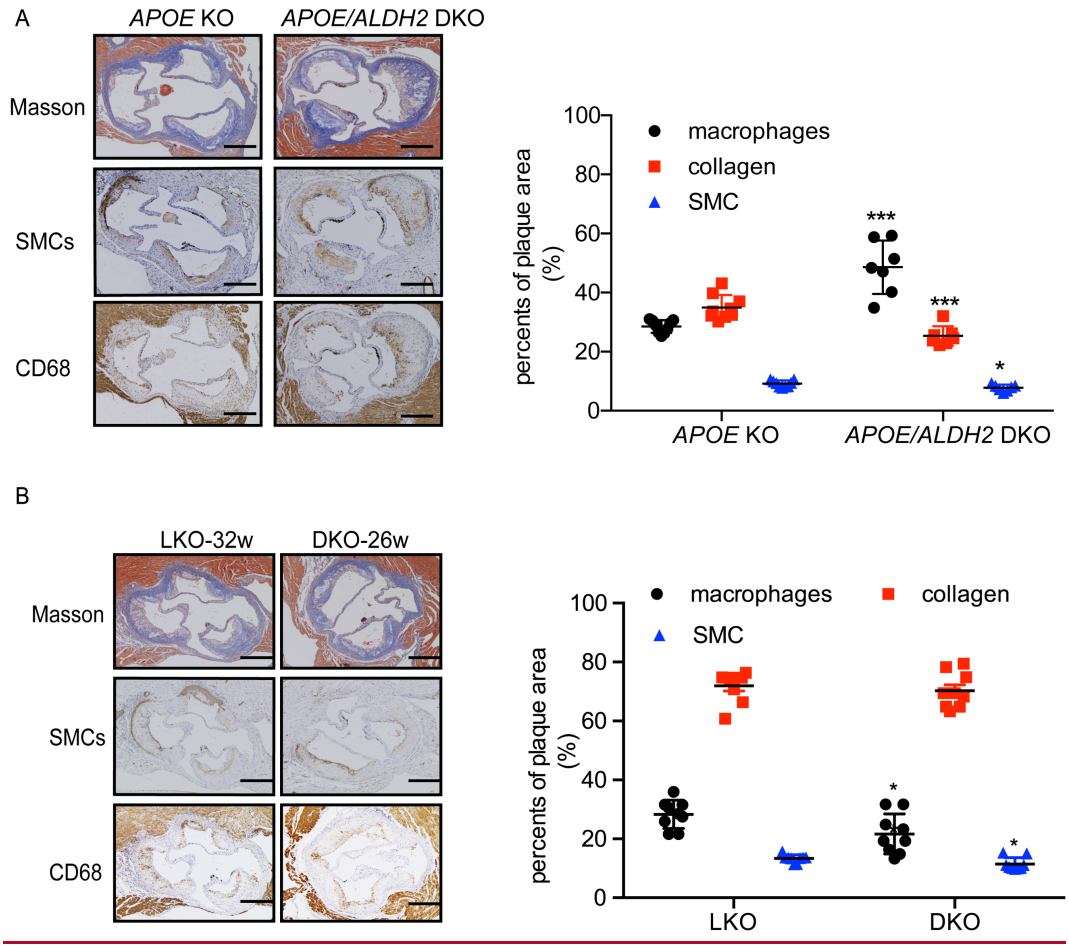

Supplemental Figure S2. IHC staining results from ALDH2 KO mice in LKO and APOE background. A, representative IHC and quantification of macrophages, collagen, and SMCs after 12 weeks in *APOE* and *APOE/ALDH2* DKO mice (n=8-9). Scale bar, 400μm. **B,** representative IHC and quantification of macrophages, collagen, and SMC after 26 weeks of WD feeding in LKO and *ALDH2/ LDLR* DKO mice (n=9). Scale bar, 400μm. ~~representative IHC and quantification of macrophages, collagen, and SMCs after 12 weeks (n=8-9) . Scale bar, 400μm.~~ Statistical comparisons were made using 2-tailed Student's t test. All data represent mean ± SD. *P < 0.05, **P < 0.01, ***P < 0.001.

Figure S3

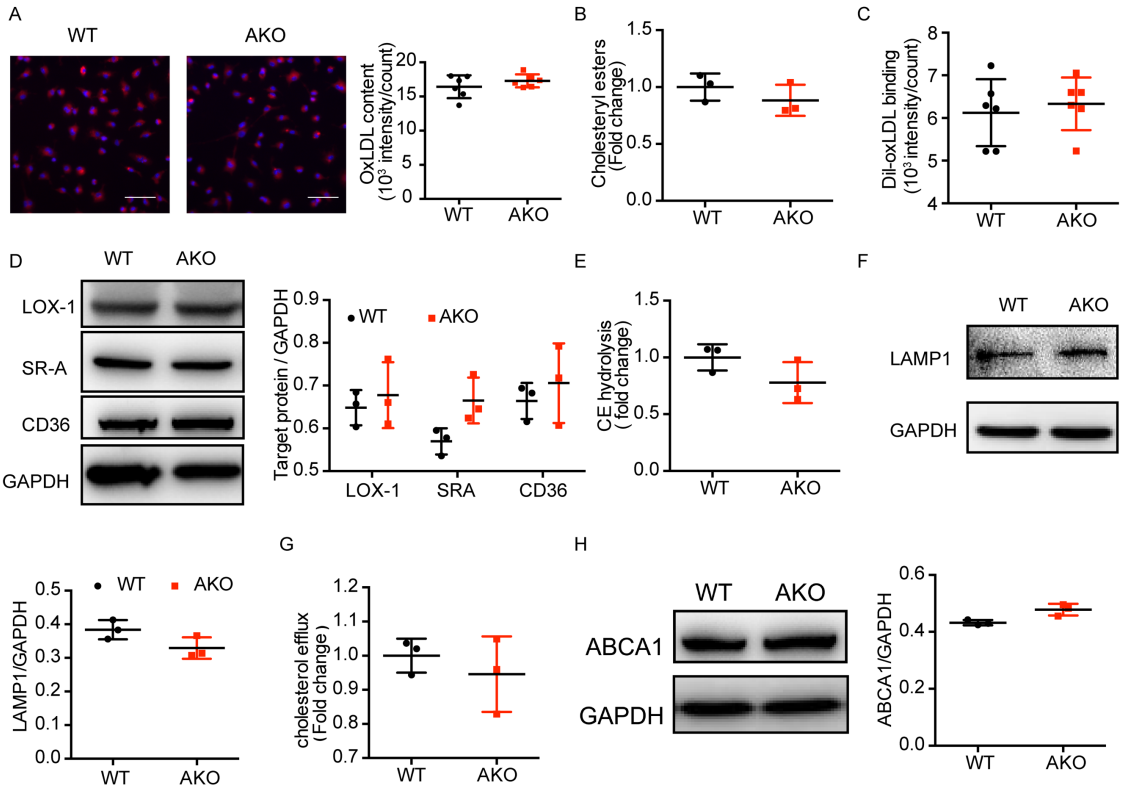

Supplemental Figure S3~~2~~. Comparing to WT, *ALDH2* KO does not affect lysosomal function, CE hydrolysis, and foam cell formation. A, *ALDH2* knockout does not changed foam cell formation in WT BMDMs and quantification (n=6). The oxLDL signals are shown in red and Hoechst signals are shown in blue. Scale bar, 100 μm. **B**, Levels of CE do not change in *ALDH2* KO BMDMs comparing to WT macrophages (n=3). **C,** binding to ox-LDL in WT and *ALDH2* KO BMDMs (n=6). **D,** expressions of LOX-1, SRA, and CD36 in WT and *ALDH2* KO BMDMs (n=3). **E**, CE hydrolysis does not change in *ALDH2* KO BMDMs comparing with WT macrophages (n=3). **F,** expression of lysosome function marker -LAMP1 in macrophages of WT and ALDH2 KO macrophages (n=3). **G,** cholesterol efflux is similar in *ALDH2* KO and WT BMDMs (n=3). **H,** ABCA1 expression in WT and AKO BMDMs (n=3). ~~All data represent mean ± SEM.~~Statistical comparisons were made using 2-tailed Student's t test. All data represent mean ± SD. ~~*P < 0.05, **P < 0.01, ***P < 0.001.~~

Figure S~~43~~

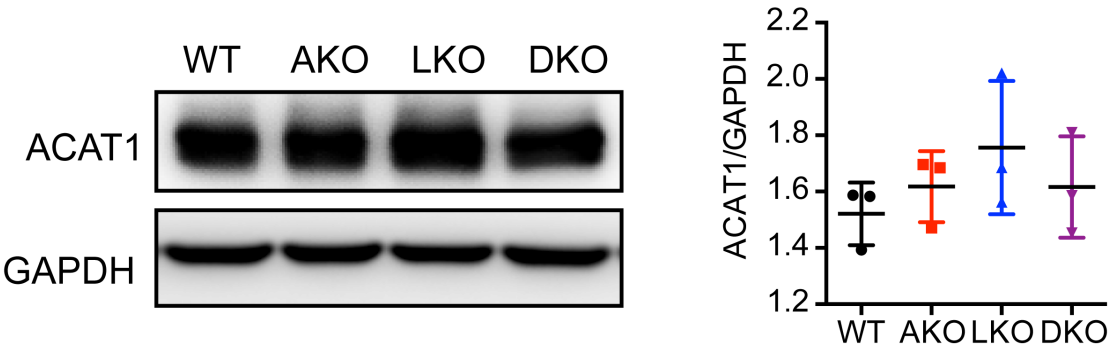

Supplemental Figure S~~43~~. No significant changes in ACAT1 expression in WT, *ALDH2* KO (AKO), *LDLR* KO (LKO) and *LDLR/ALDH2* DKO (DKO) macrophages. ~~**A,**~~ ACAT1 expression in WT, AKO, LKO and DKO macrophages. Statistical comparisons were made using ANOVA. All data represent mean ± ~~SEM~~SD.

Figure S54

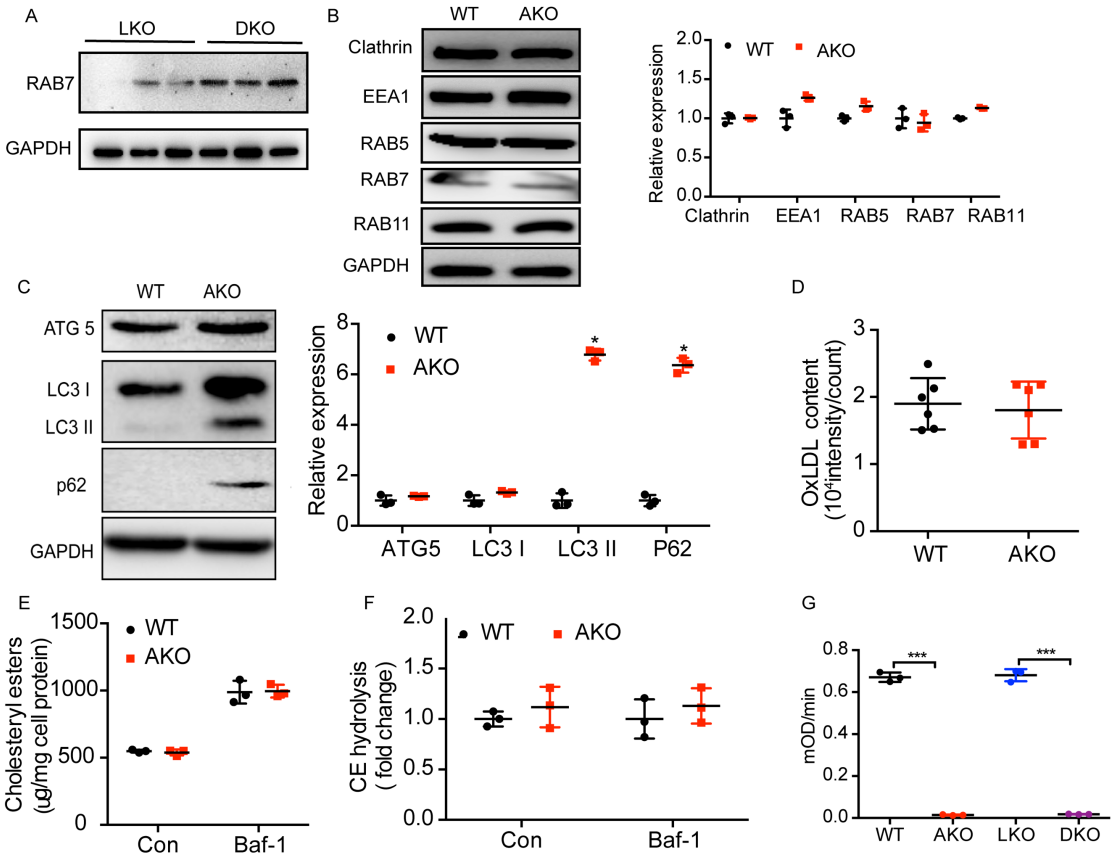

Supplemental Figure S54. Endocytosis and foam cell formation do not change but autophagy ~~decreased~~ decreases in *ALDH2* KO macrophages comparing to WT macrophages. A, RAB~~ab~~7 expression in LKO and DKO macrophages with oxLDL treatment (n=3). ~~**B,** representative confocal results for autophagic flux in *ALDH2/LDLR* DKO macrophages and *LDLR* KO macrophages. Scale bar, 5 μm.~~ **B~~C~~,** endocytosis is not changed in AKO and WT macrophages (n=3). **C~~D~~,** autophagic flux decreased in AKO macrophages comparing to WT (n=3). **D~~E~~ to F~~G~~,** inhibition of autophagy by bafilomycin A1 treatment does not change foam cell formation (D~~D~~, n=6), cholesterol ester accumulation (E~~E~~, n=3), and CE hydrolysis (F~~F~~, n=3) of in AKO macrophages. **G~~H~~,** ALDH2 enzymatic activity in WT, AKO, LKO and *ALDH2/LDLR* DKO macrophages (n=3). Statistical comparisons were made using 2-tailed Student's t test (B, C, D, E and F) or ANOVA (G). All data represent mean ± SD~~SEM~~. *P < 0.05, ~~**P < 0.01,~~ ***P < 0.001.

Figure S~~6~~5

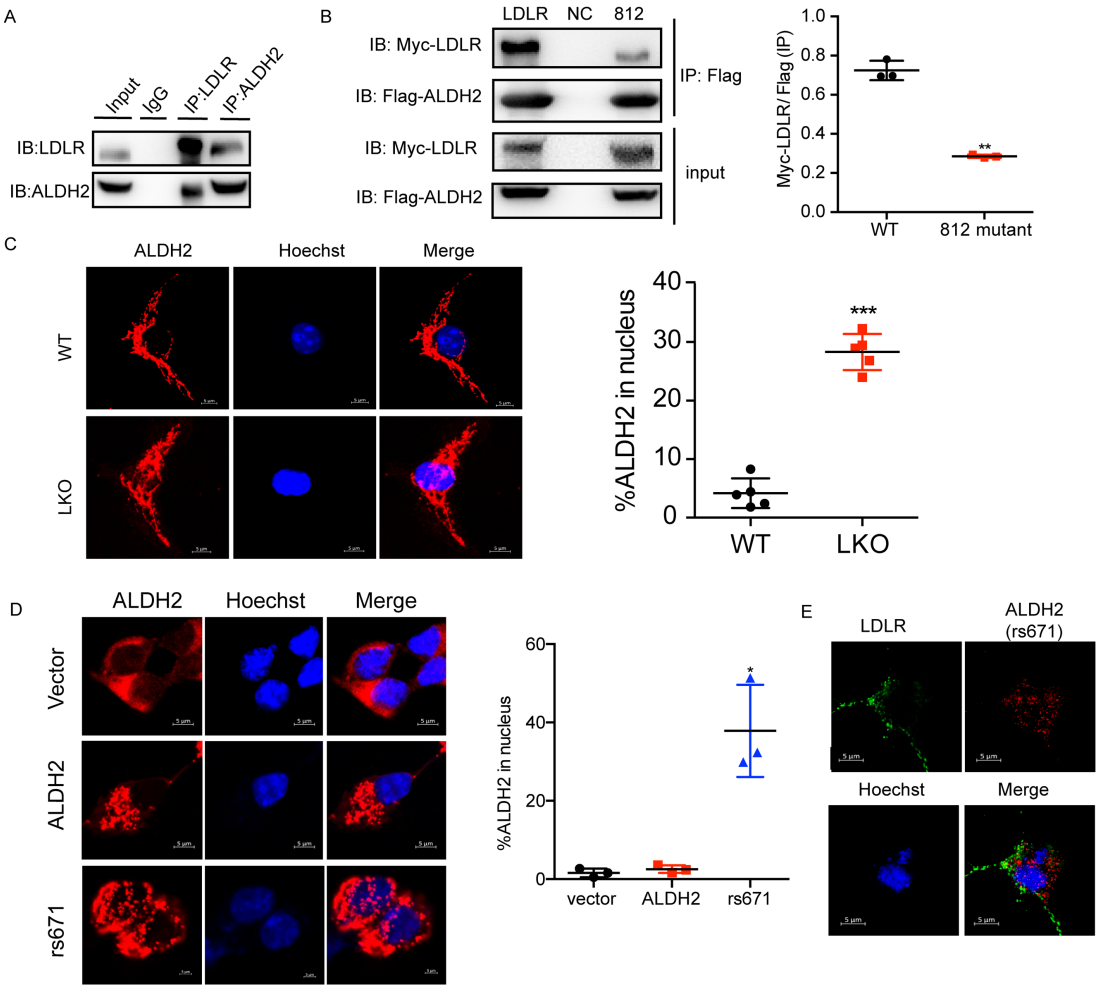

Supplemental Figure S~~6~~5. LDLR and ALDH2 rs671 mutant play an important role in AMPK-mediated ALDH2 translocation. A, LDLR directly interacts with ALDH2 in 293T cells. **B,** LDLR C-terminal mutant (N812A) ~~decreased~~ decreases the binding to ALDH2 in 293T cells (n=3). **C,** LDLR KO increases ALDH2 translocation to nucleus and quantification (n=5). Scale bar, 5 μm. **D,** ALDH2 rs671 promotes the translocation of ALDH2 to nucleus demonstrated by immunofluorescence (n=5, Scale bar, 5 μm). **E,** ALDH2 rs671 mutant translocates to the nucleus even with the over-expression of LDLR (293T cells, Scale bar, 5 μm). Statistical comparisons were made using 2-tailed Student's t test (B and C) or ANOVA (D). All data represent mean ± SD. *P < 0.05, **P < 0.01, ***P < 0.001. ~~**B,** the expression of LDLR in LKO macrophages blocks the translocation of ALDH2 to nucleus. Scale bar, 5 μm. **C,** ALDH2 rs671 mutant translocates to the nucleus even with the over-expression of LDLR (293T cells, Scale bar, 5 μm). **D,** proteomics identifies one phosphorylation of ALDH2 by AMPK in LKO macrophages treated with Metformin: T356. **E,** MS identification of ALDH2~~

~~phosphorylation site at Y148 in LDLR KO macrophages. **F,** ALDH2 rs671 mutant pulls down more AMPK compared to WT ALDH2 (n=3). **G,** a gene-dose upregulation of LDLR inhibits the phosphorylation of ALDH2. All data represent mean ± SEM. *P < 0.05, **P < 0.01, ***P < 0.001.~~

Figure S~~6~~7

A

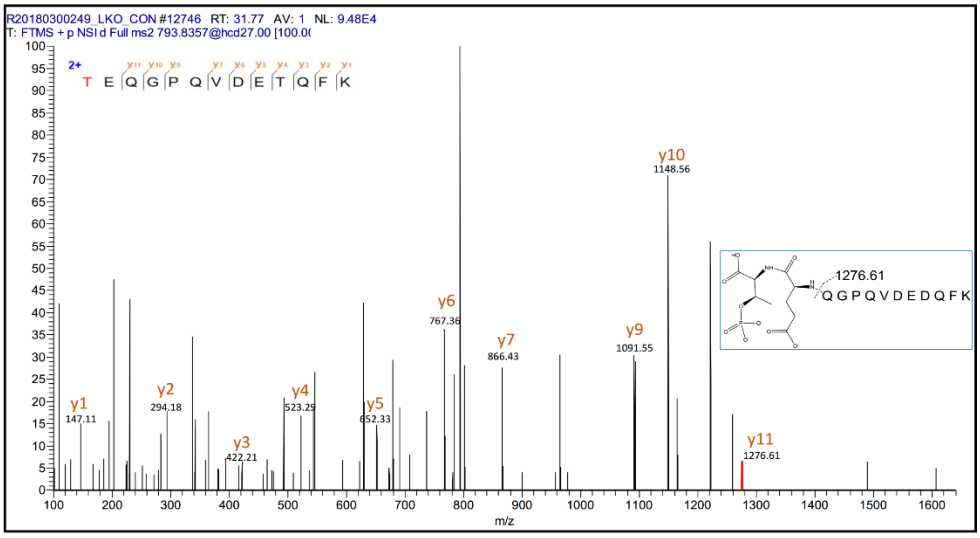

B

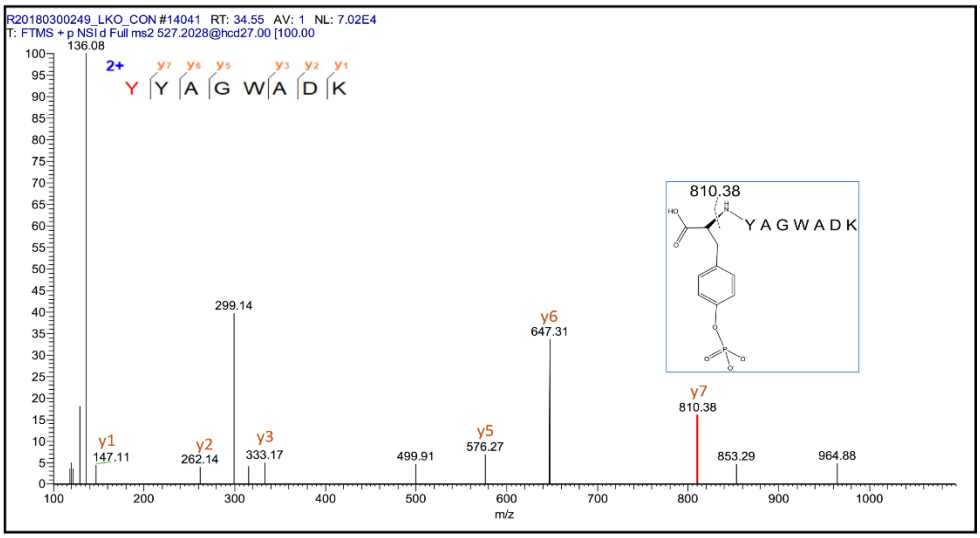

Supplemental Figure S~~6~~7. Proteomics results for identifying two phosphorylated sites of ALDH2 by AMPK in LKO macrophages. A, the phosphorylated site of ALDH2 by AMPK in LKO macrophages treated with Metformin - T356. **B,** MS identification of ALDH2 phosphorylation site at Y148 in *LDLR* KO macrophages.

Figure S~~8~~7

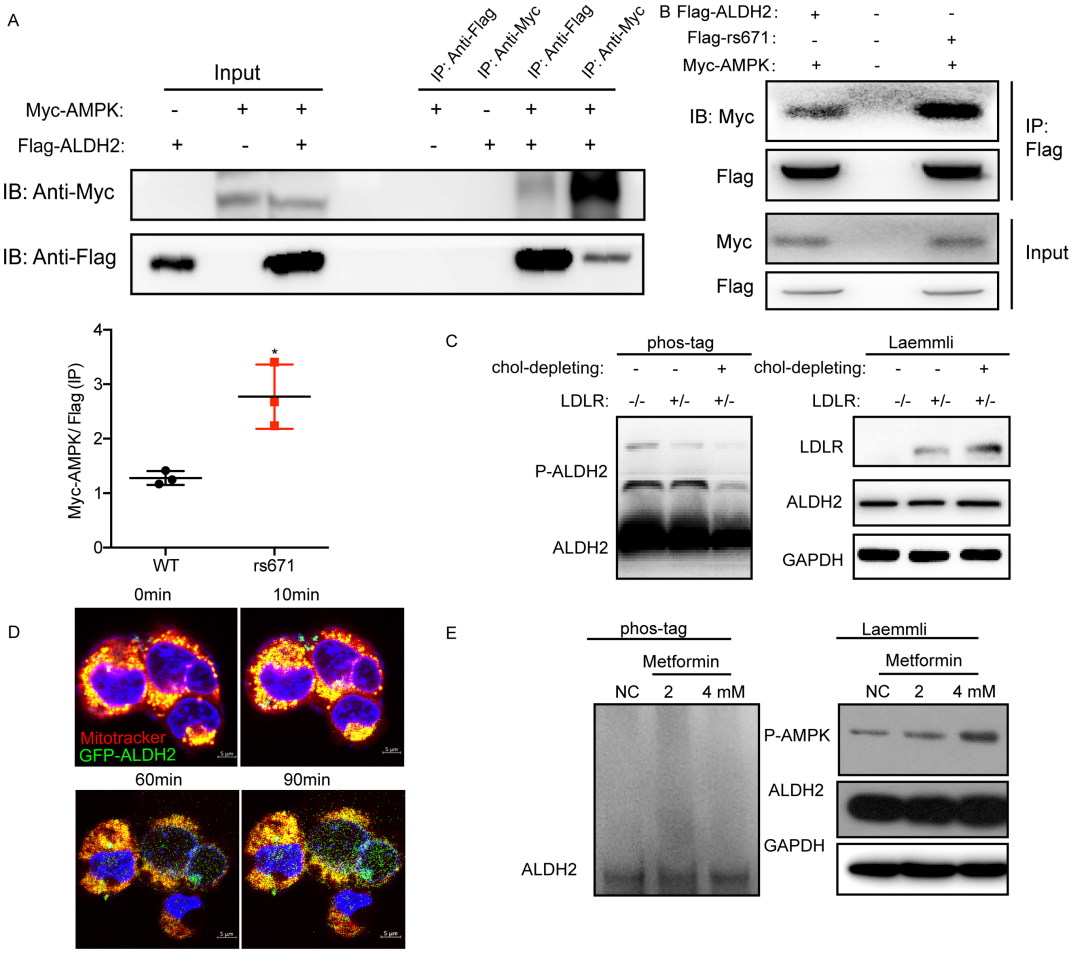

Supplemental figure S~~8~~7. AMPK promotes ALDH2 translocation through phosphorylating ALDH2 in the absence of LDLR. ~~Compound C decreased the phosphorylation of AMPK in WT BMDMs. All data represent mean ± SEM. **P < 0.01.~~ A, ALDH2 directly binds to AMPK in 293T cells. **B,** ALDH2 rs671 mutant pulls down more AMPK compared to WT ALDH2 (n=3). **C,** a gene-dose upregulation of LDLR inhibits the phosphorylation of ALDH2. **D,** AMPK activation by AICAR promotes ALDH2 nuclear translocation by immunofluorescence in 293T cells (Scale bar, 5 μm). **E,** dose-dependent activation of AMPK does not change ALDH2 phosphorylation in the present of LDLR in WT BMDM by SuperSep™ Phos-tag™ SDS-PAGE. Statistical comparisons were made using 2-tailed Student's t test. All data represent mean ± SD. *P < 0.05, **P < 0.01, ***P < 0.001.

Figure S~~8~~9

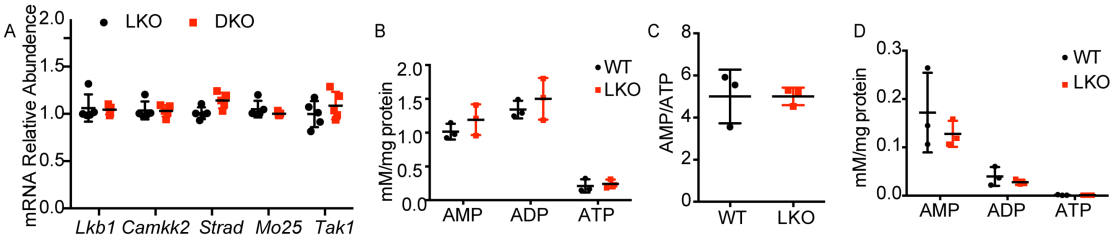

Supplemental Figure S~~8~~9. ~~**P62 transcriptional level in WT and LDLR KO BMDMs with AMPK activation or inhibition. A,** p62 mRNA level in LDLR KO BMDMs treated with Compound C and Metformin (n=3). **B,** p62 mRNA level in WT BMDMs treated with Compound C and Metformin (n=3).~~ ***ALDH2* KO does not affect the expression of the upstream genes of AMPK and the levels of AMP, ADP, ATP in LDLR KO BMDMs. A,** the qPCR analysis results of the expression of the upstream of AMPK in *LDLR/ALDH2* DKO BMDMs and LDLR KO BMDMs (n=5). **B to C,** the levels of AMP, ADP, ATP (B) and ratio of AMP/ATP (C) in WT and LKO BMDMs (n=3). **D,** AMP, ADP, ATP levels in LKO and WT BMDMs treated with oxLDL (n=3). Statistical comparisons were made using 2-tailed Student's t test. All data represent mean ± SD. ~~*P < 0.05, **P < 0.01, ***P < 0.001.~~

Figure S10~~9~~

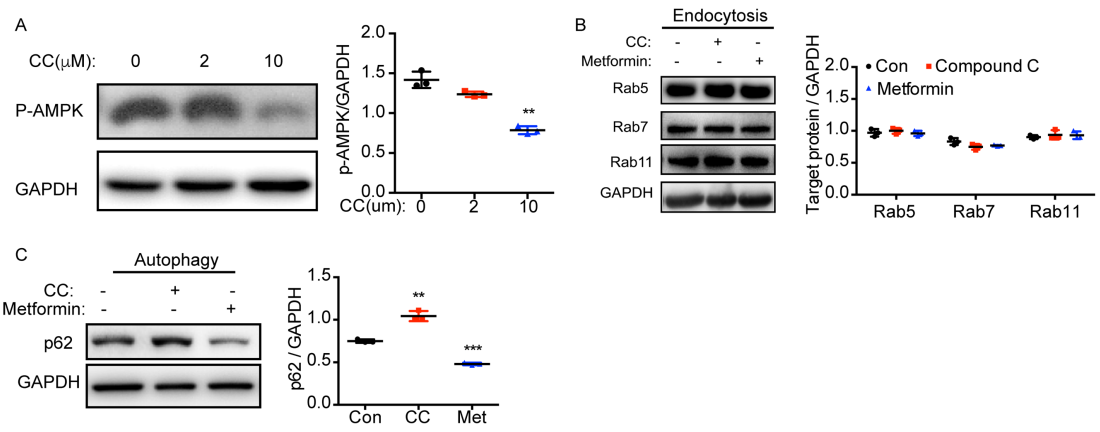

Supplemental Figure S10~~9~~. AMPK regulates autophagy without affecting ~~does not affect~~ endocytosis ~~and increased autophagy~~ in WT BMDMs. A, Compound C decrease~~d~~s the phosphorylation of AMPK in WT BMDMs (n=3). **B to C,** AMPK activation by Metformin increases autophagy (C, n=3)~~.~~, whereas AMPK inhibition by compound C ~~leads to~~ decrease~~d~~s autophagy without affecting endocytosis (B, n=3). Statistical comparisons were made using ANOVA. All data represent mean ± SD. *P < 0.05, **P < 0.01, ***P < 0.001.

Figure S1~~0~~

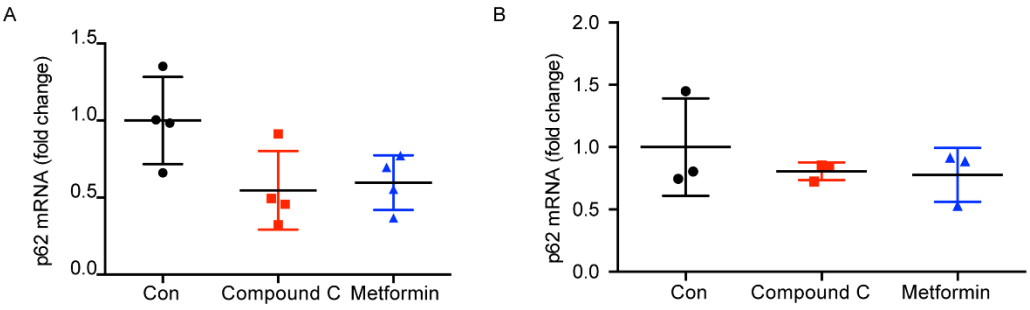

Supplemental Figure S1~~0~~. Transcriptional levels of *p62* ~~transcriptional level~~ in WT and *LDLR* KO BMDMs with AMPK activation or inhibition. A, *p62* mRNA level in LDLR KO BMDMs treated with Compound C and Metformin (n=4). **B,** *p62* mRNA level in WT BMDMs treated with Compound C and Metformin (n=3). Statistical comparisons were made using ANOVA. All data represent mean ± SD. ~~*P < 0.05, **P < 0.01, ***P < 0.001.~~

.

Figure S12~~1~~

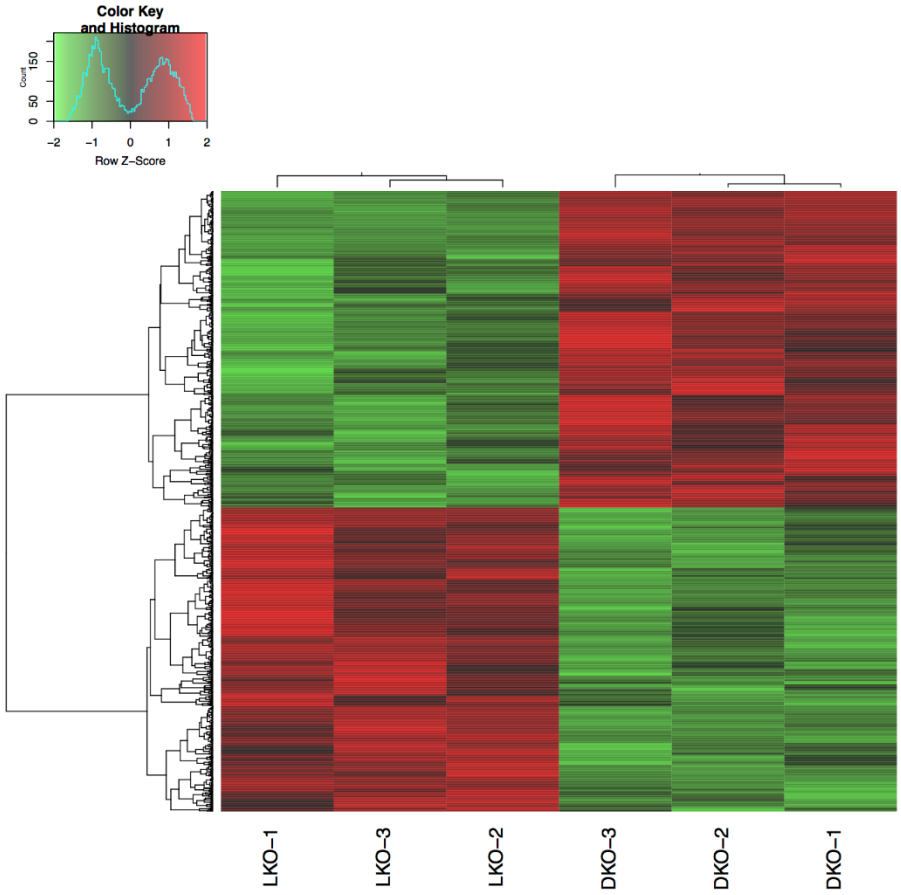

Supplemental Figure S12~~1~~. ~~h~~Heat map of the clustering of differentially expressed genes (DEGs) transcripts ~~expression~~ in LKO and DKO BMDMs.

Figure S13

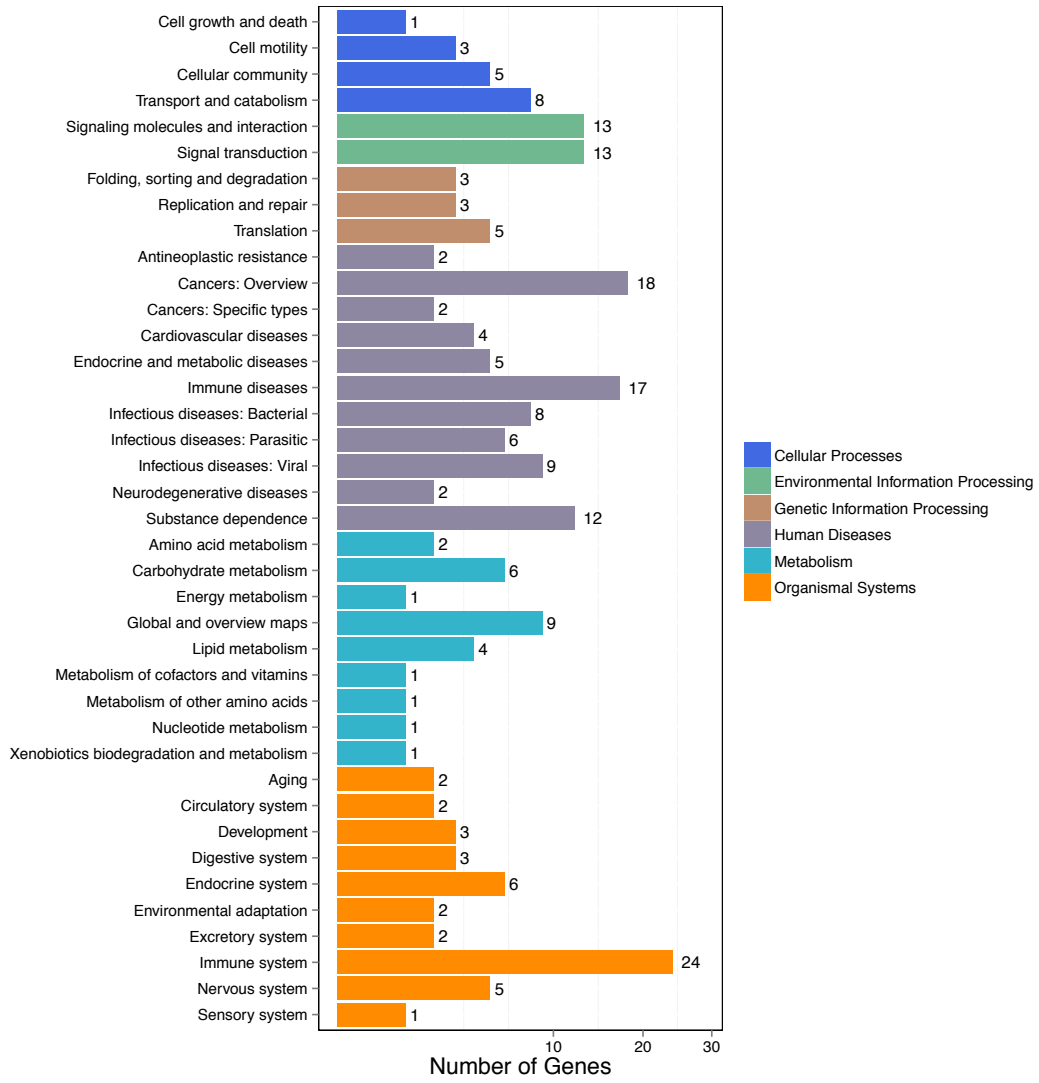

Supplemental Figure S13. Numbers of DEGs in different biological pathways from LKO and DKO BMDMs were analyzed by using Noiseq method.

Figure S14

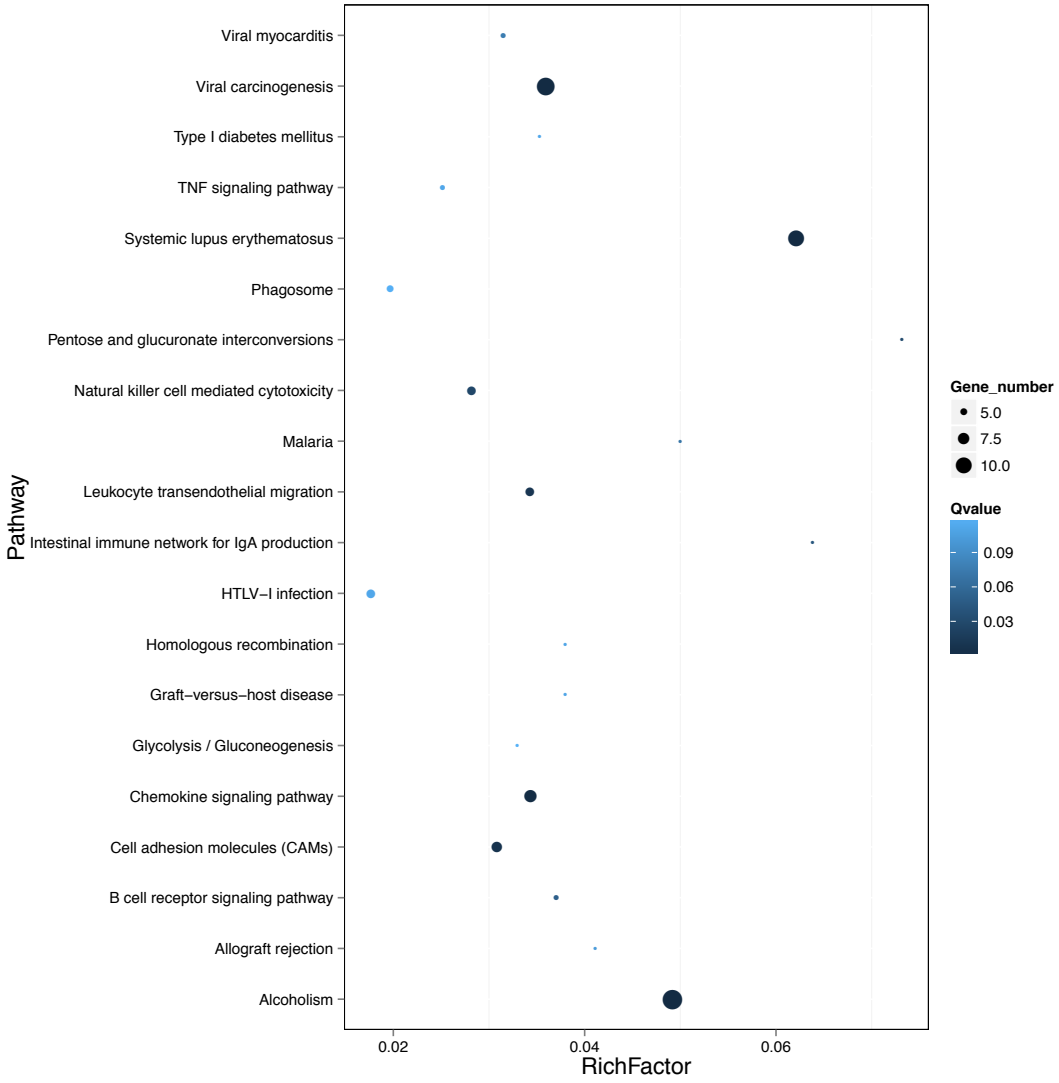

Supplemental Figure S14. The pathway enrichment analysis from DEGs in LKO and DKO BMDMs.

Figure S15

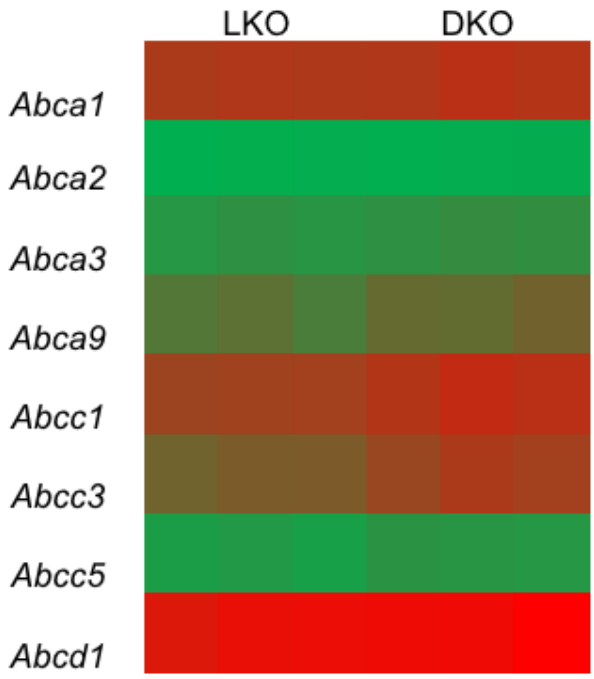

Supplemental Figure S15. The expression of transporter genes in LKO and DKO BMDMs from RNA-seq transcriptomic results.

Figure S16

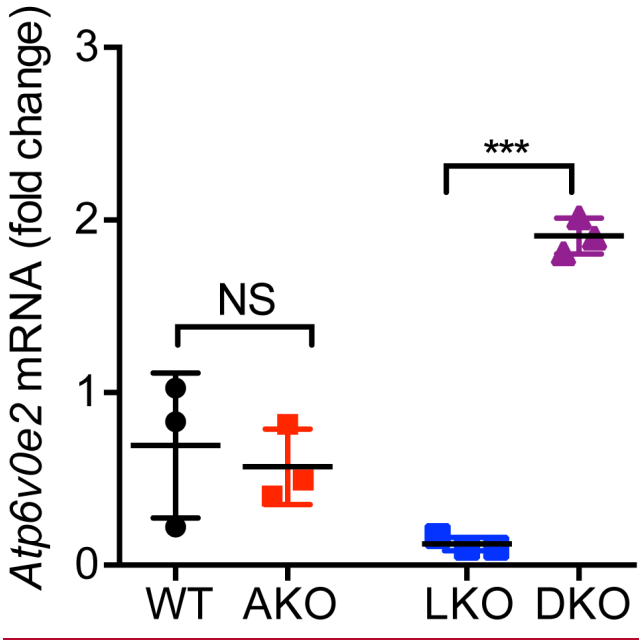

Supplemental Figure S16. *ALDH2/LDLR* DKO leads to a significant upregulation of mRNA level of *Atp6v0e2* comparing with LKO (n=3).

Figure S17

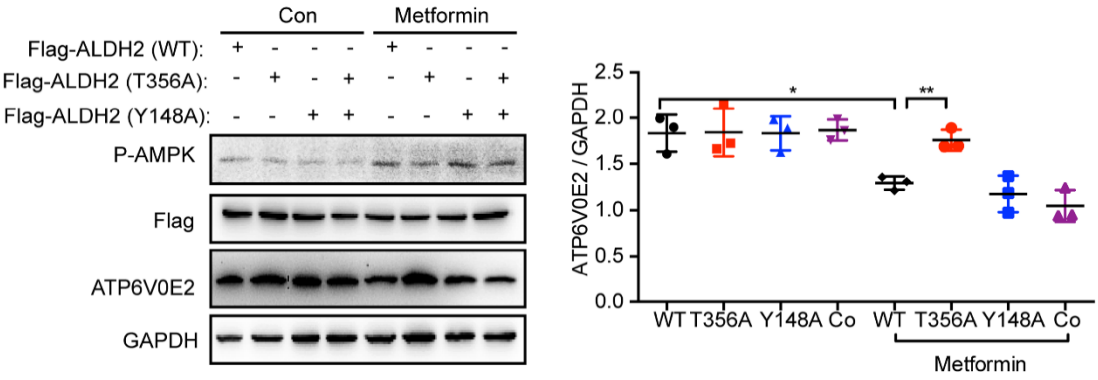

Supplemental Figure S17. *ALDH2* T356A mutant not Y148A mutant rescues decreased ATP6V0E2 expression in the presence of Metformin (n=3). Statistical comparisons were made using ANOVA. Data represent mean ± SD. *P < 0.05, **P < 0.01, ~~***P < 0.001~~.

Figure S18

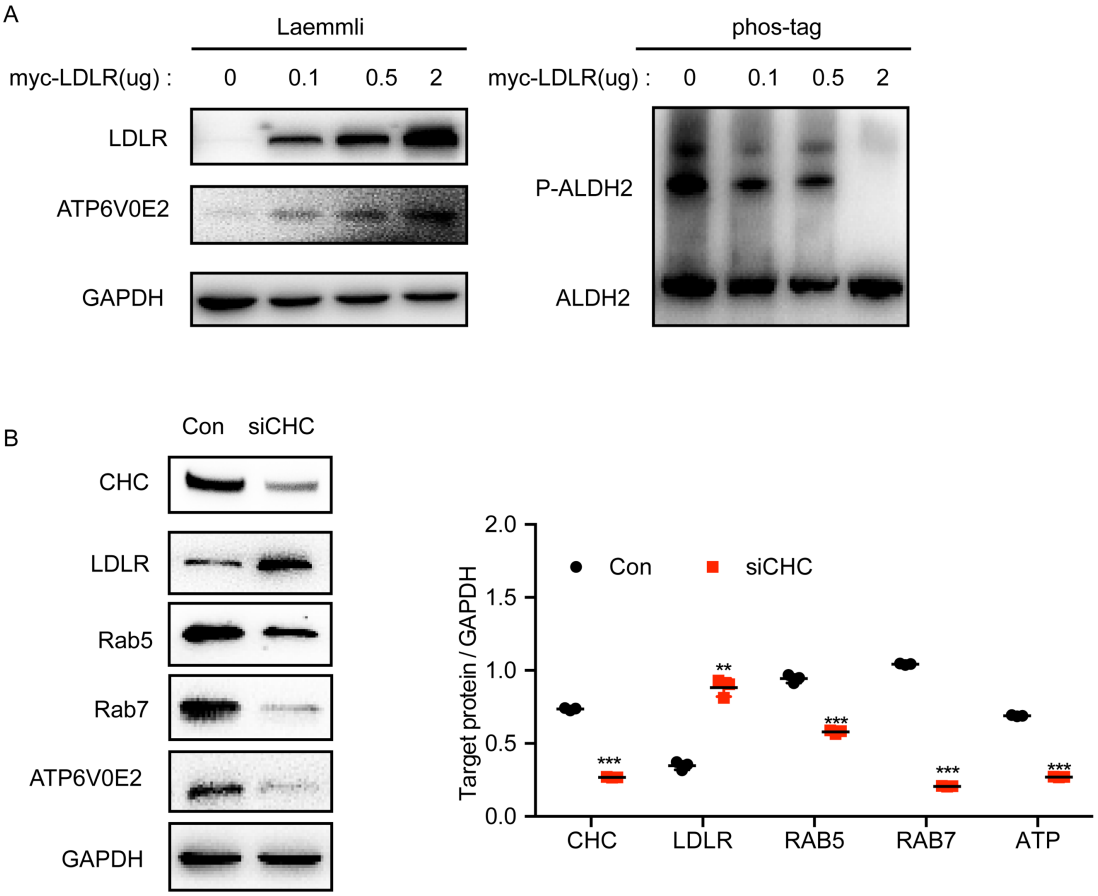

Supplemental Figure S18. LDLR is important for regulating ATP6V0E2 expression. A, LDLR gene-dose dependently increaseds ATP6V0E2 expression and decreaseds ALDH2 phosphorylation. **B,** the inhibition of endocytosis decreaseds ATP6V0E2 expression by silencing Clathrin heavy chain in 293T cells (n=3). Statistical comparisons were made using 2-tailed Student's t test (C) or ANOVA (A). All data represent mean ± SD. ~~*P < 0.05,~~ **P < 0.01, ***P < 0.001.

Figure S19

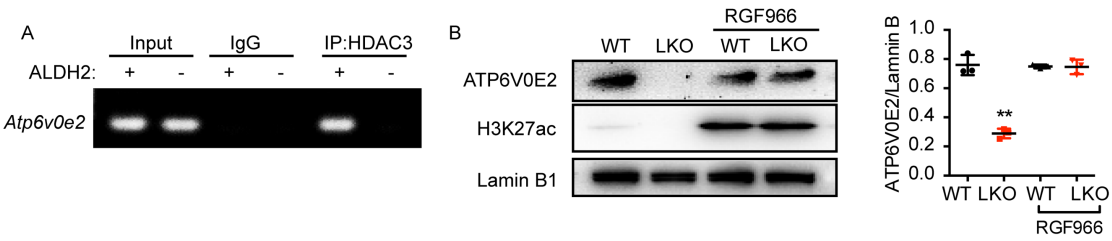

Supplemental Figure S19. ALDH2 decreases *Atp6v0e2* transcription through interaction with HDAC3. A, ChIP assay demonstrate~~d~~s that in the absence of LDLR, ALDH2 promote~~d~~s the binding of HDAC3 to *Atp6v0e2* promoter in BMDMs treated with Metformin. **B**, HDAC3 inhibitor RGF966 diminishe~~d~~s the decreased expression of ATP6V0E2 in LKO macrophages (n=3). Statistical comparisons ~~were~~are made using ANOVA. All data represent mean ± SD. *P < 0.05, **P < 0.01, ***P < 0.001.

Figure S20

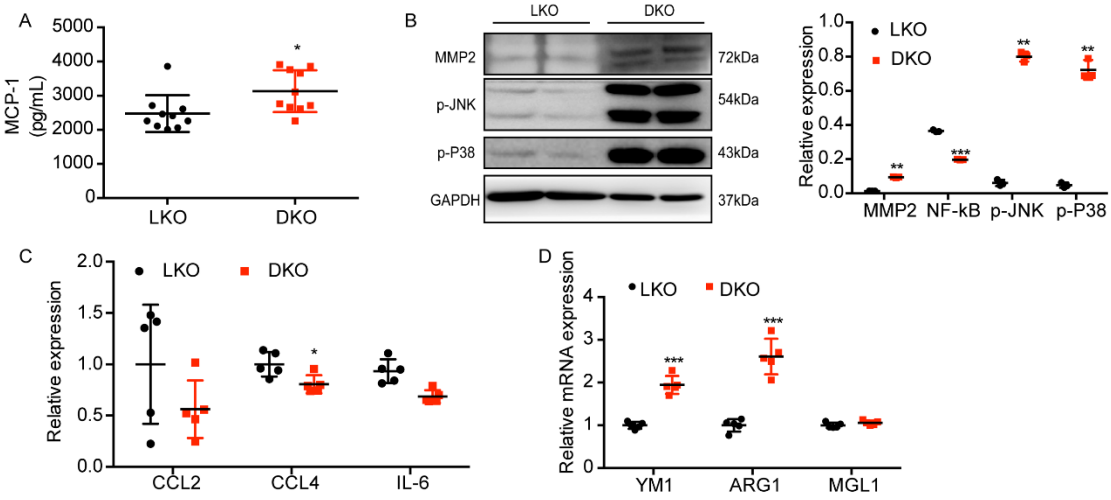

Supplemental Figure S20. Inflammation is ~~increased~~elevated in plasma, primary endothelial cells from *LDLR/ALDH2* DKO mice; Polarization toward anti-inflammation in *LDLR/ALDH2* DKO macrophages. A, MCP-1 expression increase~~d~~s in plasma from LDLR/ALDH2 DKO comparing with LDLR KO mice (fed WD 26w, n=10). **B,** MMP2, p-JNK and p-P38 are significantly increased in LDLR/ALDH2 DKO mice (n=3). **C,** mRNA levels of M1 markers (CCL2, CCL4 and IL-6) decrease~~d~~ in LDLR/ALDH2 DKO BMDMs treated with LPS (n=5). **D,** mRNA levels of M2 markers (YM1, ARG1 and MGL1) in LDLR/ALDH2 DKO BMDMs treated with IL-4 (n=5). Statistical comparisons were made using 2-tailed Student's t test. All data represent mean ± SD. **P < 0.01, ***P < 0.001.

Supplemental Table

Supplemental tTable 1.

log_2Ratio (DKO/LKO)	Symbol	Description
11.2	*Gm8580*	ribosomal protein L29 pseudogene
10.9	*Ifi44l*	interferon-induced protein 44 like
9.7	***Atp6v0e2***	**ATPase, H+ transporting, lysosomal V0 subunit E2**
7.9	*Hist1h2ba*	histone cluster 1, H2ba
7.8	*Hist2h3c1*	histone cluster 2, H3c1

Supplemental tTable 1. *Atp6v0e2* ranks at the top 3 most upregulated DEGs in BMDMs of *LDLR/ALDH2* DKO.

Supplemental ~~table~~ Table 2~~1~~.

Primers required for PCR.

Gene	Forward	Reverse
Camkk2	CTGGCAACTGTGATCCTGGT	CTTGCTTCCTTGGGCTCAGA
Lkb1	CAGTGCCTGGTGTCGAGGAG	CTACACTAAAGCCCCAAACCCC
Mo25	GGTTGCCATGAAAGAAATTCTGT	AGCTGTGCTACGGCCTCTGT
Strad	ATGGAGTCCAAGCTACTCTGC	GAAGCAAGATCATTAGAGAACCTCA
Tak1	ATGGAGTCCAAGCTACTCTGC	GAAGCAAGATCATTAGAGAACCTCA
Lox-1	ACAAGATGAAGCCTGCGAAT	GCTGAGTAAGGTTCGCTTGG
Cd36	TGCTGGAGCTGTTATTGGTG	TGGGTTTTGCACATCAAAGA
Sra	TCACTGGATGCAATCTCCAA	ACGTGCGCTTGTTCTTCTTT
ATP6V0E2	GATACCCCACCTGAGCATCG	CACAGCAGGGCATAAGAGGTA
L32	TTAAGCGAAACTGGCGGAAAC	TTGTTGCTCCCATAACCGATG
ALDH2	GCCGGATCCATGTTGCGCGCTGCC GCCCG	GCCCTCTAGATTATCAGGCGTCATCAGC GTCCTTGTAGTCCTCGAGTGAGTTCTTC TGAGGCACTT
ALDH2(rs671)	CGGGCTGCAGGCATACACTGAAGTG AAACTGTCACAGTCA	TGACTGTGACAGTTTTCACTTCAGTGTAT GCCTGCAGCCG
LDLR(Myc)	GGCCAATTGATGGGGCCCTGGGGC TGGAA	GCTCTAGATCACAGATCCTCTTCTGAGAT GAGTTTTTGTTCCGCCACGTCATCCTCC AGAC
LDLR(His)	GGCCAATTGATGGGGCCCTGGGGC TGGAA	GCTCTAGATTAGTGGTGGTGGTGGTGGT GCGCCACGTCATCCTCCAGAC

Supplemental Table 3.

Top 3 GO functional classifications on overlapping DEGs in *LDLR*$^{-/-}$ and *ALDH2*$^{-/-}$*LDLR*$^{-/-}$ BMDMs.

Category	Accession	GO_term	*p* value	Genes
CC	GO:0009986	cell surface	1.12E-06	*Cd19, H2-Q8, H2-Eb1, Cxcr4, Ccr7, Btla, Cd79a, Ms4a1, H60a, Ly6a, H2-Q7, Vcam1*
	GO:0044421	extracellular region part	0.02335	*Saa3, Iigp1, Apln, Sorl1, C4b, Gbp2b,Gm6644, Mgp, Cxcl14, Wfdc21, Chil1, Ccl24, Cmtm8, Vcam1, Orm2*
	GO:0005576	extracellular region	0.02628	*C4b,Gbp2b, Apln, Sorl1, Saa3, Iigp1, Ccl24, Orm2, Cmtm8, Vcam1, Mgp, Wfdc21, Chil1, Cxcl14, Gm6644*
MF	GO:0046983	protein dimerization activity	0.00398	*Eno3, Hist2h2aa2, Ugt1a6b, Ikzf3, Hist1h2br, Hist1h2bq, Adora2a, Hist1h2bj, Itgb2l, Hist1h2be*
	GO:0003823	antigen binding	0.0048	*H2-Q7, H2-Q8, H2-Eb1*
	GO:0001637	G-protein coupled chemoattractant receptor activity	0.32597	*Cxcr4,Ccr7*
BP	GO:0002376	immune system process	1.34E-06	*C4b, Oasl1, Mzb1, Cxcr4, Itgb2l,H2-Eb1, H60a, Slfn1, Ccl24,Vcam1, Irf7, Orm2, Cxcl14,12482_Ms4a1,22780_Ikzf3, Ifi44l, Gbp2b, H2-Q8, Mylpf, Cd19, Ccr7, Adora2a, Sox4, H2-Q7, Cd79a*

	GO:0046649	lymphocyte activation	3.78E-05	*Vcam1, Slfn1, H60a, Cd79a, Ms4a1, Ikzf3, Sox4,Itgb2l, H2-Eb1, Adora2a, Cxcr4, Ccr7, Mzb1*
	GO:0046651	lymphocyte proliferation	0.00017	*Ikzf3, Ccr7, Mzb1, H2-Eb1, Itgb2l, Slfn1, Vcam1*

Detailed DEGs in top 3 DEGs in biological process (BP), cellular component (CC) and molecular function (MF) from microarray results.

Supplemental Table 4.

Clinical characteristics of human subjects recruited in the clinical studies

	ALDH2*1 **(n=16)**	***ALDH2*2/2*1*** **(n=10)**	**p-value**
Age(years)	26.00 ± 0.87	25.90 ± 1.06	0.94
Male gender(%)	62.5	60	
Triglycerides (mmol/L)	1.08 ± 0.17	1.31 ± 0.21	0.40
Total cholesterol(mmol/L)	4.10 ± 0.16	4.26 ± 0.21	0.56
HDL-C(mmol/L)	1.39 ± 0.13	1.37 ± 0.13	0.90
LDL-C(mmol/L)	2.48 ± 0.13	2.7 ± 0.2	0.48
APOA1(g/L)	1.14 ± 0.07	1.15 ± 0.06	0.90
APOB(g/L)	0.81 ± 0.05	0.87 ± 0.07	0.53
APOE(mg/L)	39.81 ± 3.48	41.72 ± 3.94	0.72

*ALDH2*1, ALDH2* wild type; *ALDH2*2/2*1, ALDH2 SNP* (rs671) heterozygous. Values are mean ± SEM. HDL-C, high density lipoprotein (HDL) cholesterol; LDL-C, low density lipoprotein (LDL) cholesterol; APOA1, apolipoprotein A1; APOB, apolipoprotein B; APOE, apolipoprotein E. Statistical analysis was conducted by using an unpaired Student's t test.

Detailed method

Bone Marrow Transplant

For bone marrow transplant experiments, 8-week old recipient mice (*ALDH2*$^{-/-}$*LDLR*$^{-/-}$ or *LDLR*$^{-/-}$) were irradiated with 9 Gy (Gammacell 40 Cs γ-irradiation). Bone marrow from donor mice (*ALDH2*$^{-/-}$*LDLR*$^{-/-}$ or *LDLR*$^{-/-}$) were harvested by flushing the femurs and tibias with RPMI-1640 cell medium (Catalog No. SH30809.01, Hyclone, USA). Then red blood cells were removed by using Red Blood Cell Lysis Buffer (8.3g ammonia chloride, 1g potassium acid carbonate, 0.37g Disodium EDTA in 1L H_2O). Single-cell suspensions were prepared by filtering the cells through a 70 μm cell strainer (Catalog No.352350, BD, Breda). Then, cell suspensions were centrifuged at 3000 ×g for 6 min. Supernatant was removed and re-suspended with 1x PBS (pH 7.4). Next, $2x10^6$ donor bone marrow cells were injected into the tail vein of irradiated recipient mice. The mice were fed neomycin sulfate water (0.5g/L) for 8 weeks to allow full bone marrow reconstitution. After recovery, chimeric mice were fed western diet for 12 weeks. At the end of each experiment, aorta was harvested and genotyping PCR analysis for the corresponding genes (ALDH2 or LDLR) was conducted on tail (receptor) and blood white cells (donor) to ensure the BMT results.

Analysis of Aortic Lesions

After sacrificing adult mice, we separated the aorta and fixed in 4% paraformaldehyde overnight at 4 °C. After the aorta was washed for 3 mins by using 70% ethanol, atherosclerotic plaque was stained for 6 mins by using 0.5% Sudan IV (Catalog No. S100286, Aladdin, China) and washed twice for 3 mins by using 80% ethanol. Aorta was washed with PBS (pH 7.4). Finally, the adventitial fat was removed and the aorta was opened longitudinally and pinned onto black wax by using Minutien Pins (catalog no.26002-10, Fine Science Tools, USA). Digital images were analyzed with the ImageJ software (Version 1.47, National Institutes of Health, Bethesda, MD).

Bone Marrow-Derived Macrophages (BMDMs)

Bone marrow cells were flushed from tibia and femur with RPMI-1640 (Hyclone, USA). Next, red blood cells were removed by adding 3mL red blood cell lysis for 5 mins. And the reaction was stopped by adding 30mL PBS (pH7.4). The BMDMs became single-cell suspension by flowing through 70 μm cell filters (BD, Breda) and were centrifuged at 3000 ×g for 6 min. Finally, we resuspended cells in RPMI-1640 (Hyclone, USA) medium supplemented with 20% FBS (Catalog No. A31604-01, Gibco Life Technologies, USA), penicillin and streptomycin (Catalog No.15140-122, Gibco Life Technologies, USA) and 30 % filtered L929 cell-conditioned medium as a source of M- CSF. Cell medium was changed every 2 days and the cells were cultured for 7 days to allow differentiation into BMDMs.

Phagocytotic Assay

After differentiation, BMDMs were plated on 24 wells plate and grew overnight. Then, we incubated BMDMs in 37℃ for detecting ox-LDL content or 4℃ for binding with 10 μg/ml Dil-oxLDL (Catalog No. YB-0010, Yiyuan Biotechnologies, China) for 4 hours or 50ug/mL ox-LDL (Catalog No. YB-002, Yiyuan Biotechnologies, China) for 6 hours. Then, BMDMs were washed with 1x PBS three times and fixed with 4% paraformaldehyde for 1 hour. Cell nuclei were stained with Hoechst (1 μg/ml, Catalog No. H6024, Sigma-Aldrich, USA) for 10 min and ox-LDL was stain with Nile red at room temperature. Cells were washed and re-suspended with PBS. Then, cells were imaged and assessed by Thermo Fisher Cellomics ArrayScan Infinity HCS system (Thermo Fisher Scientific, Waltham, MA). The images were analyzed by Thermo ScientificTM StoreTM Express Image and Database Management Software. For drug treatment experiments, 1 mM AICAR (Catalog No. S1802, Selleck, USA) or 10 mM Bafilomycin-A (Catalog No. S1413, Selleck, USA) was added to medium for 1 hours before adding Dil-oxLDL or ox-LDL.

Detection of Phosphorylated ALDH2 in SuperSep^{TM}Phos-tag^{TM} SDS-PAGE

SuperSep™Phos-tag™ SDS-PAGE (Catalog No.198-17981, Wako, Japan) was used for detection of phosphorylated ALDH2 in BMDMs. Protocol in this method was the same as normal SDS-PAGE except phos-tag PAGE gel was soaked in 1x transfer buffer with 10mM EDTA for a minimum of 20 minutes with gentle agitation for 3 times and then soaked in 1x transfer buffer (without EDTA) for 10 minutes with gentle agitation before transferring proteins to PDVF membrane. Then PDVF membrane was blocked by 5% BSA and blotted with anti-ALDH2 (Catalog No. 15310-1-AP, Proteintech, USA).

Nuclear and Cytoplasmic Fractionation

BMDMs were rinsed with ice-cold PBS, and lysed on ice in lysis buffer supplemented with complete protease inhibitor cocktail (Catalog No. B14001, Biotool, USA). Then, separating the cytoplasmic and nuclear proteins was conducted by using the NE-PER nuclear and cytoplasmic extraction kit (Catalog No. P0027, Beyotime, China) according to the manufacturer's instructions.

Cholesterol Efflux Assay

BMDMs firstly were treated with 15μg/ml chol-d7 for 24h. After washing the cells thoroughly with PBS, 50μg/ml HDL was added to induce cholesterol efflux. After incubating 24h, media were collected for GC-MS and 10% BMDMs proteins were collected for quantification.

Free cholesterol extraction

BMDMs were treated with 15μg/ml cholesterol-d7 (chol-d7) for 24h. 10% BMDMs were used to measure protein concentration by the BCA assay. Free cholesterol was extracted by using 2ml hexane: IPA (3:2, v/v) supplemented with 1% acetic acid and 6μg 5α-cholestane as internal standard (IS). After vortex and centrifugation, the upper organic phase was collected. Then the remaining liquid was extracted again with hexane. Finally, after organic phase was dried under nitrogen, 40ul of pyridine and 40ul of derivatizing agent (BSTFA + TMCS) for GC-MS analysis were added. The standards contained IS used for quantification were treated by using the same methods. This extraction method is used for cholesterol efflux assay.

Gas chromatography and mass spectrometry (GC-MS)

GC-MS was performed in the EI mode using Shimadzu GC-MS QP2010. The ion source temperature was set at 230°C while the injection temperature was set at 250°C. The cholesterol TMS derivatives were separated on an Rxi-5MS column (19m, 0.25mm inner diameter, 0.25μm film thickness). The initial GC oven temperature was set at 110°C， increased to 250°C by 30°C/min for 1min, and then increased 10°C/min to 280°C for 1min followed by 3°C/min to 300°C for 3min. The GC chromatograms were extracted at m/z = 217 and 357 for IS, m/z=336, 375, 465 for chol-d7. The retention time (RT) for IS and cholesterol were about 13.8 min and 17.4min respectively. Then peak areas were integrated using the instrument software. Calibration curves were generated using chol-d7 and IS. The final results were normalized to cell lysates protein.

Hydrolysis of Cholesteryl esters

Macrophages were incubated with 50 μg/mL ox-LDL with or without 5nM Balfmycin-A1 for 20h. Cholesteryl esters were extracted by adding 4mL hexane: IPA (3:2, v/v) and 3μg cholesteryl esters (19:0) as internal standard (IS). After vortex and centrifugation, the upper organic phase was collected. Then, after organic phase was dried under nitrogen, 50ul of hexane for LC-MS analysis were added. Normal phase LC was carried out with Agilent 1260 Quat pump VL and Accela 1250 pump. The column was Phenomenex 3-μm silica (2 mm × 250 mm). The samples were run at a flow rate of 200μL/min in mobile [0.5% IPA in hexane]. Eluent from all normal-phase methods was modified with 4mM NH_4OAc in IPA at a flow rate of 200μL/min. And then all the solvents were introduced to the ion source at a flow rate of 400μL/min. The MS was performed on a TSQ Vantage (Thermo Fisher Scientific). The MS was operated in positive ion and multiple reaction monitoring (MRM) mode. Chromatographic peaks

were integrated and area ratios (samples *versus* IS) were generated using Xcalibur (Thermo Scientific, San Jose, USA). CEs changing (hydrolysis) is expressed as fold change relative to control, calculated as follows[4]: % hydrolysis = (CE1 – CE2)/(CE1) *100, where CE1 represents cholesteryl esters after treating with ox-LDL for 20h, and CE2 represents cholesteryl esters after the macrophages were incubated for 20 h with 50 μg/mL HDL; fold change = (% hydrolysis sample/% hydrolysis control).

Retrovirus (TRV)

After incubating LDLR knockout BMDMs for 7 days, 5μg/mL polybrene and 100μL $5*10^7$ TU/mL HBhTRV-m-LDLR-3xflag-GFP in 900 μL cell medium (RPMI-1640+10% Gibico FBS) were added. After incubating BMDMs at 37 °C for 4 hours, we added 1mL cell medium (RPMI-1640+10% Gibico FBS) with 5 μg/mL polybrene. Cell medium was changed after incubating 24 hours at 37 °C and then BMDMs were incubated 48 hours.

Immunoprecipitation (IP)

For BMDMs, 10cm dishes of BMDMs (grown to 80%-90% confluence) for immunoprecipitating specific protein (ALDH2, LDLR, AMPK, HDAC1-3) were collected and lysed with 800 μl per dish of ice-cold cell lysis buffer added with protease inhibitor cocktail (Biotool, USA). Cell lysates were incubated with respective antibodies (1:500 for ALDH2 antibody, 1:50 for AMPK antibody, 1:50 for LDLR antibody, 1:50 for HDAC1-3 antibody) and rotated slowly overnight at 4°C. Then, overnight protein aggregates were added with protein A/G beads (1:10 for IP, catalog no. B23202, Biotool, USA) and rotated slowly overnight at 4°C. The beads were washed with 300 μL wash buffer for 3 times at RT and then mixed with 50 μL 1x loading buffer for immunoblotting.

For 293T cells, 10cm dishes of 293T cells (grown to 60% confluence) transfected with specific tag protein (flag-ALDH2, myc-AMPK, myc-LDLR or his-LDLR) 48 hours by using Attractene Transfection Reagent (Catalog No. 301005, Qiagen, Germany) was collected and lysed with 800 μl per dish of ice-cold cell lysis buffer added with protease inhibitor cocktail. Then, cell lysates were directly incubated with myc-beads or flag-beads (1:10 for IP, Catalog No. B26301 for myc-beads, Catalog No. B23102 for flag-beads, Biotool, USA) overnight at 4°C. Next, the beads were washed 3 times with 500 μL TBS and mixed with 50 μL 1x loading buffer for immunoblotting. The band intensities on developed films were quantified using Image J software.

Fluorescence Microscopy[1]

BMDMs were grown on glass coverslips in 6-well dishes and were cultured to 60–80% confluence. Next, Cells were washed with PBS and fixed with 1mL ice-cold methanol for 5 mins at room temperature. They were rinsed twice with 1 ml PBS for 5 mins (room temperature) and then permeated with 1 ml of 1% Triton X-100 (diluted in PBS) for 5 min at room temperature. Cells were washed twice for 5 mins with 1 ml PBS and were blocked with 1mL 1%BSA for 30 mins. Next, BMDMs were incubated with primary antibodies (anti-ALDH2, Catalog No. 15310-1-AP, Proteintech, USA) 30 mins at 37 °C. The cells were then rinsed three times with 1 ml PBS, and then incubated with Alexa-Fluor 555-conjugated anti-rabbit secondary antibody (Catalog No.4413S, Cell signaling Technology, USA; diluted 1:100 in PBS) for 30mins at 37°C in the dark. They were washed four times with 1 ml PBS, and then mounted on slides by using DAPI (Catalog No. P36935, Life technologies, USA). Cells were imaged under a Zeiss LSM 780. Thresholds were set automatically by the software.

RNA-Seq Analysis

$LDLR^{-/-}$ and *$ALDH2^{-/-}LDLR^{-/-}$*BMDMs were lysed with TRIzol reagent. The library preparation and sequencing were carried out by Beijing Genomics Institute BGI (Wuhan, China). We measured the expression of the transcripts isoforms by using RSEM and used NOISeq method to screen differentially expressed genes (DEGs) between two groups. Top 3 GO functional classifications on overlapping DEGs showed in supplemental **Table 3.** Heat maps were conducted by using the R software.

Chromatin Immunoprecipitation (ChIP Assay)

LDLR$^{-/-}$ and WT BMDMs (5×10^6) cultured in 10cm plates were pretreated with or without 1mM AICAR for 1 h. ChIP assay was conducted by using ChIP Assay kit (Catalog No. 17-295, Millipore, USA). Then, the cells were fixed with 1% formaldehyde for 10 min at 37°C. After removing the cell media, the cells were washed twice with cold PBS containing 1mM PMSF and lysed with 200uL SDS lysis buffer. The lysates were sonicated on a 4 mins of "9 second on and 15-second off" cycle to produce chromatin fragments of 100–500bp. The sonicated lysates were centrifuged for 10 mins at 13,000 rpm at 4°C and transfer the supernatant to a new 2mL-tube. After diluted 10-fold in ChIP dilution buffer and incubated with Protein G Agarose for 60 min at 4°C with rotation to reduce non-specific binding, the supernatants were incubated with mouse anti-ALDH2 antibody (1:500, Proteintech) or normal mouse IgG (1:500) at 4°C overnight. The Protein G Agarose was used to collect the antibody-antigen-DNA complexes. For input samples, 10% sample DNA was used. The immunoprecipitated material was washed sequentially with Low Salt Immune Complex Wash Buffer, High Salt Immune Complex Wash Buffer, LiCl Immune Complex Wash Buffer, TE, and Elution Buffer. All samples were incubated with 0.2 M NaCl at 65°C overnight followed by proteinase digestion at 45°C for 2 h to separate DNA from protein/DNA complexes. Eluted DNA was further purified using PCR purification kit (Qiagen) and subjected to qRT-PCR analysis using the primers showed in supplemental **Table 2**.

Detection of Autophagic Flux

LDLR$^{-/-}$ and *ALDH2*$^{-/-}$*LDLR*$^{-/-}$ BMDMs ($3\text{x}10^5$) were plated and grew overnight on 20 mm glass bottom cell culture dish (Catalog No.801001, NEST, USA) in RPMI-1640 (10% Gibico FBS). The fusion of autophagosomes and lysosomes in BMDMs in control and Bafilomycin A1 (Baf) (1nM) treated cells was detected using the PremoTM Autophagy Tandem Sensor RFP-GFP-LC3B Kit (Catalog No. P36239, Thermo Fischer Scientific, USA). Firstly, BMDMs were added 15μL RFP-GFP-LC3B sensor for 11 hours in RPMI-1640 (10% Gibico FBS) and then treated with Bafilomycin A1 or DMSO for 12 hours with 50μg/mL ox-LDL. Then, cells were washed with PBS and stained nuclear with Hoechst, finally resuspended with RPMI-1640 cell medium. RFP-GFP-LC3B sensor enables the detection of LC3B positive, neutral pH autophagosomes in green fluorescence (GFP) and LC3B positive acidic pH autophagolysosme in red fluorescence (RFP). Fluorescent images were taken by using confocal microscopy (Carl Zeiss Meditec, Inc.). LC3B positive autophagosomes (yellow) and LC3B positive autophagolysosome (red) were analyzed and quantified by using Image J software.

Plasmids

Flag tagged human *ALDH2* and *ALDH2 (rs671)* mutant were constructed into pcDNA3.0 vector through the restriction sites BamHI and XhoI. Primer is showed in **Table 2**. Amplified product was recovered using PCR clean-up kit and digested with restriction enzyme DpnI before transfected into competent cells (DH5α strain). Clones were picked and amplified to be sequenced in order to confirm the mutation construction.

Myc and 6xHis tagged Human LDLR were also constructed into Vector pcDNA3.0 via restriction sites MfeI and XbaI. pcDNA 3.0 vector was digested with EcoRI and XbaI, Fragments that were amplified via PCR were digested with XbaI. Ligation was performed by T4 ligase and ligation products were transfected into competent cells (DH5α strain). Primer is showed in **Table 2**. Clones were picked and amplified to be sequenced to verify the final results.

Statistical Analysis

Results were expressed as mean ± SEM or mean ± SD from at least three independent experiments by using GraphPad Prism 5. Statistical analysis was conducted by using an unpaired Student's t test or two-way ANOVA. A two-tailed probability value of < 0.05 was considered statistically significant. *$p < 0.05$; **$p < 0.01$; ***$p < 0.001$.